

A Numerical Study of Shock Formation in Cylindrical and Two-Dimensional Shock Tubes

By

Nobuyuki SATOFUKA*

Summary: Shock formation process and shock tube performance are investigated numerically. Numerical method applied is FLIC method proposed by Gentry, Martin and Daly for solving compressible fluid flows. A model of diaphragm opening process which does not base on the usual one-dimensional assumption is presented. Four cases for cylindrical shock tubes and one for two-dimensional were calculated for diaphragm pressure ratios of 100 and 1000. Diaphragm opening times were varied from about 100 to 500 μ sec. Shock formation process predicted from present calculations shows a qualitative agreement with experimental results. Shock tube performance was also calculated and compared with those predicted by ideal shock tube theory and other models such as formation-from-compression model proposed by White and multi stage model proposed by Ikui and Matsuo. Presented result shows a close agreement with that predicted by multi stage model.

1. INTRODUCTION

Most theoretical studies on shock tube flows have been based upon the usual ideal model which assumes; (1) one-dimensional flow, (2) ideal nonviscous, non-heat conducting driver and driven gases and (3) instantaneous diaphragm removal [1],[2]. According to these assumptions, wave speeds and the flow properties of the uniform states are readily determined from the initial conditions in terms of the specific heat ratios of driver and driven gases, diaphragm pressure ratio and initial temperature ratio. Schematic diagrams of this model are illustrated in Fig. 1.

In practice, however, it is not possible to remove instantaneously the diaphragm which separates high and low pressure chambers. Photographic investigations have revealed that the process by which a diaphragm actually ruptures involves formation of a small opening near the center, followed by the outward tearing of the material and the folding back of the leaves so formed. The effective cross-sectional area of the shock tube at the diaphragm location therefore increases gradually with time instead of attaining its maximum value instantaneously as assumed in the usual ideal analysis. Associated with this fact, a constant strength shock wave is not formed immediately but a train of compression waves generated by the

* Kyoto Technical University, Faculty of Industrial Arts. Dept. Mechanical Engineering.

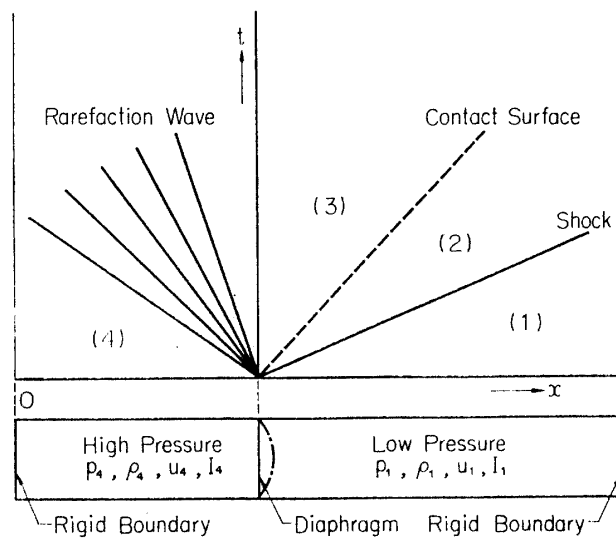


FIG. 1. Schematic diagrams of flow in a shock tube.

gradual opening of the diaphragm are sent out and overtake each other to form a weak shock wave. Then this shock wave is continuously accelerated by succeeding compression waves and finally attains its stationary speed.

White [3] has suggested a model which has taken into account this effect of finite opening time of the diaphragm. His model has assumed, instead of above-mentioned assumption (3), that diaphragm opening time is finite and continuously sent out unsteady compression waves all overtake the first wave at the same point to form a shock wave. When the same driver and driven gases such as air/air are selected, for a given diaphragm pressure ratio his theory always predicts a shock Mach number greater than that given by ideal shock tube theory. His model, however, does not include the effects of shock acceleration process.

Ikui and Matsuo [4] have extended White's model to take into account of this process of shock acceleration. Their model (multi stage model) has based upon the assumptions that continuous compression waves sent out through the diaphragm opening process can be divided into a finite number of groups, each of which is represented by a single compression wave, and a weak shock wave formed by the coalescence of such compression waves belonging to the first group is accelerated stepwise by succeeding compression waves. According to this model, still higher shock Mach numbers than White's model are predicted for the case of the larger diaphragm pressure ratios.

These two models still base on the one-dimensional assumption. As mentioned above, actual diaphragm opening process is not one-dimensional and analysis taking into account of this not-one-dimensional effects has not yet been performed.

In the present work, the process of shock formation in cylindrical and two-dimensional shock tubes is investigated numerically using the Fluid-in-Cell (FLIC) method [5]. A model of the diaphragm opening process not assuming one-dimensionality and computational cycle of FLIC method is described in some detail and results for shock formation distances and shock tube performance

are presented and discussed. FORTRAN programme used in this calculation is listed in appendix. Present calculations were performed on HITAC 5020 Fs at Institute of Space and Aeronautical Science, University of Tokyo and at National Aerospace Laboratory.

NOTATION

| | |
|---------------|---|
| c ; | speed of sound |
| CPUT; | computational time |
| D ; | hydraulic diameter of shock tube |
| E ; | fluid energy per unit volume |
| I ; | specific internal energy |
| IN ; | maximum number of cells in x -direction |
| $IN1$; | maximum number of cells in x -direction in high pressure chamber |
| $IN2$; | maximum number of cells in x -direction in low pressure chamber |
| JN ; | maximum number of cells in r (or y)-direction |
| M_s ; | shock Mach number |
| MEMSTP; | parameter controlling the diaphragm opening time |
| N ; | maximum time cycle number |
| P, p ; | static pressure |
| r ; | coordinate perpendicular to shock tube axis of symmetry |
| t ; | time |
| u ; | velocity in x -direction |
| v ; | velocity in r (or y)-direction |
| x ; | coordinate parallel to shock tube axis of symmetry |
| x_f ; | shock formation distance |
| y ; | coordinate perpendicular to shock tube axis of symmetry in two-dimensional case |
| γ ; | specific heat ratio |
| ΔM ; | mass flowing across cell boundary during the time increment Δt |
| Δr ; | cell dimension in r -direction |
| Δt ; | time increment |
| Δx ; | cell dimension in x -direction |
| Δy ; | cell dimension in y -direction |
| ρ ; | fluid density |
| τ_{op} ; | diaphragm opening time |

SUBSCRIPTS

| | |
|-------|--|
| i ; | cell number in x -direction |
| j ; | cell number in r (or y)-direction |
| n ; | time cycle number |
| 1; | initial condition of low pressure chamber |
| 2; | state compressed by the shock wave |
| 3; | state formed from the isentropic expansion of the gas in high pressure chamber |
| 4; | initial condition of high pressure chamber |

2. DIAPHRAGM OPENING PROCESS

As mentioned in the previous section, actual diaphragm opening process is three-dimensional, that is, diaphragm first ruptures from the center then follows continuous opening to full aperture. As the result a shock wave so formed by the coalescence of continuous compression waves is curved and contact surface becomes conical. Formation of compression waves in diaphragm opening process is to be considered to correspond to the rate of diaphragm opening. Therefore, to simulate this process, we must know whether it opens at an even rate or whether it opens more rapidly at some stage than others.

Campbell et al [6] has investigated experimentally the time dependence of the aperture size of rupture of aluminium diaphragms and the piercer-assisted bursting of cruciformed copper diaphragms. For both the natural rupture of an aluminium diaphragm and the piercer-assisted rupture of a copper diaphragm, a slow initiation of opening followed by a much more rapid opening to full aperture was observed. Their result shows that the time taken to 10% of full aperture was $100 \mu\text{sec}$ while that from 10% to full aperture was $80 \mu\text{sec}$ in the case of aluminium diaphragm and $750 \mu\text{sec}$ (out of $1050 \mu\text{sec}$ total) for copper. But analogous experiments for other materials have not yet been performed.

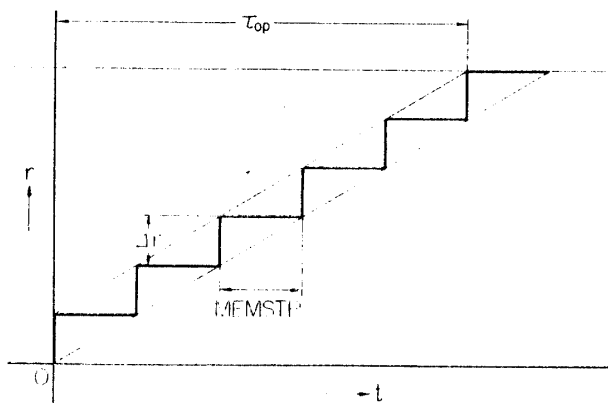


FIG. 2. Suggested model of diaphragm opening process.

In the present study, we simulate the diaphragm opening process as follows; at $t=0$, a plane diaphragm begins to rupture from the center, then stepwise increase of aperture is repeated at discrete intervals of time, MEMSTP and finally reaches to full aperture. Increment of the cross sectional area at diaphragm location is Δr or Δy , the cell dimension of r or y direction. This model of diaphragm opening process is illustrated in Fig. 2. Choosing an appropriate value of MEMSTP, we can control the rate of diaphragm opening. Throughout this calculation the values of MEMSTP are taken to be constant with time for the convenience of the calculation, therefore, rate of change of cross sectional area opened to high pressure gas is proportional to time in two-dimensional cases and to square of time in cylindrical cases.

3. CELL ARRANGEMENT AND BOUNDARY CONDITIONS

ELIC method requires a fixed (Eulerian) grid of rectangular cells of sides Δx and Δr (or Δy for two-dimensional problems) to cover the region under consideration. Fig. 3 indicates how the shock tube configuration fits into the cell system. In both cylindrical and two-dimensional problems the pair of integers (i, j) denotes the location of cell center with i and j increasing in the x and r (or y) directions, respectively and half integer indices denote the cell boundaries. IN and JN are the total number of cells in x and r (or y) directions. IN1 and IN2 indicate the number of columns of cells located in high pressure and low pressure chambers, respectively. In all cases except one, calculations were performed in cylindrical coordinates. Typical grid sizes were 400 cells in the x -direction and 10 cells in the r -direction. The plane $r=0$ was chosen as a plane of symmetry, thus there being effectively 20 cells in the r -direction. Cell dimensions were taken to $\Delta x = 2\Delta r$.

Boundary conditions on the left, the top and the bottom boundaries were set to be reflective but the right boundary was set to be continuative. Reflective boundary conditions were also set on both sides of the diaphragm not yet opened to the fluid.

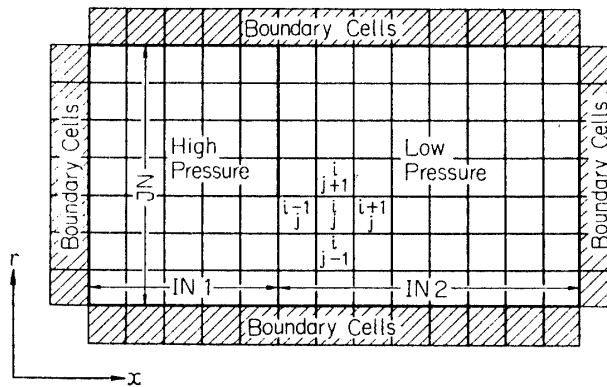


FIG. 3. The computing mesh.

4. METHOD OF SOLUTION

A number of numerical methods for time-dependent compressible flows containing shocks have been proposed. Representatives of such schemes are Lax's scheme [7], Godunov's [8] Rusanov's [9], Lax-Wendroff's [10] and Particle-in-Cell (PIC) [11]–[13] or Fluid-in-Cell (FLIC) method. Each of these schemes has characteristic properties which make it suitable for a certain class of problems. Little investigation has been performed as to which of these methods is optimum for a particular problem [14].

In the present calculations, FLIC method proposed by Gentry, Martin and Daly is chosen. The FLIC method is an outgrowth of the work of Rich [15], which is an extension of the PIC method to the case of a continuous fluid. Details of the

method can be found in references [6] and [15]. Here only an outline of the calculational cycles will be presented. The calculation of the time $(n+1)$ configuration of the fluid from that at time n proceed in cycles in which all the variables of the cell quantities are advanced to new values slightly removed from the values of the preceding cycle representing a slightly later time.

The governing partial differential equations for compressible fluid flows are as follows;

Conservation of mass,

$$\left(\frac{\partial}{\partial t} + \bar{u}\nabla\right)\rho = -\rho\nabla\bar{u} \quad (1)$$

Conservation of momentum,

$$\rho\left(\frac{\partial}{\partial t} + \bar{u}\nabla\right)\bar{u} = -\nabla p \quad (2)$$

Conservation of energy,

$$\rho\left(\frac{\partial}{\partial t} + \bar{u}\nabla\right)\left\{I + \frac{1}{2}(u^2 + v^2)\right\} = -\nabla(p\bar{u}) \quad (3)$$

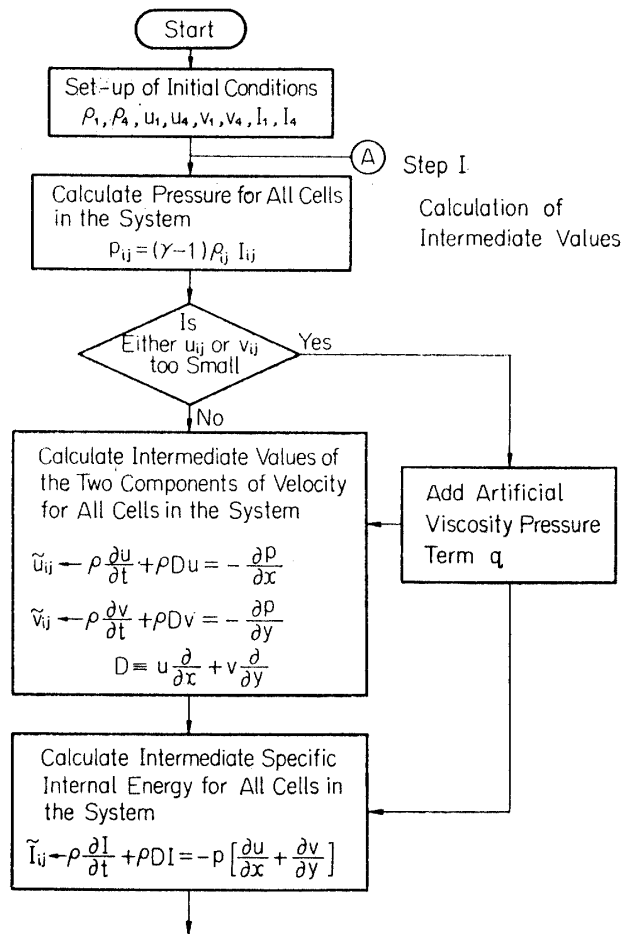


FIG. 4(a).

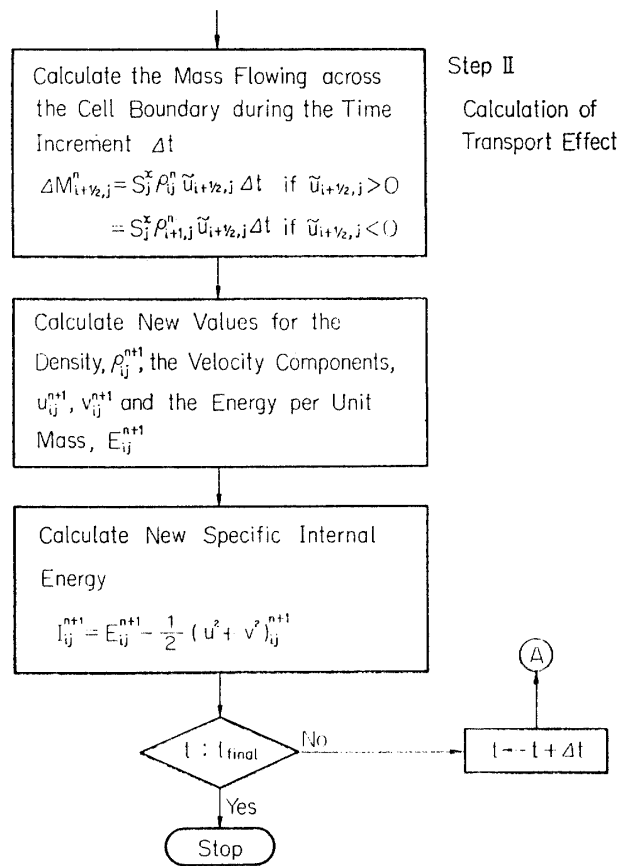


FIG. 4(b). Flow diagram of FLIC method in two-dimensional case (a) Phase I; (b) Phase II.

Equations (1), (2) and (3) are solved in two separate phases. Equation (1), that of mass conservation, may be eliminated from further consideration, as it is used only implicitly in the calculation of mass transport. Phase I treats the terms due to pressure forces only, and Phase II accounts for the remaining transport terms. Thus the second terms on the left-hand side of equations (2) and (3) are temporarily dropped in Phase I.

Briefly, Phase I begins with the calculation of new pressures for all cells from cell values of density and specific internal energy at time n or from those of initial conditions. From the gradients of these pressures are calculated tentative new values of the two components of velocity for each cell. From these new velocity components and those from the preceding cycle or from the initial condition, tentative new values of specific internal energy are computed for all cells. In both instances, the values are tentative because of omission of transport terms from the equations given above. As was seen in Phase I of the calculational cycle, only cell quantities were updated, while the fluid was assumed to be momentarily completely at rest.

In the second stage (Phase II) the term that were omitted in Phase I are accounted for, so that the cell density, momenta and energy are updated to time $(n+1)$ for the effects due to transport. Mass fluxes across cell boundaries are first computed for each cell, then mass at time $(n+1)$ is calculated for each cell

from the mass at time n and mass fluxes across four boundaries. New velocity components and specific energy are calculated from those obtained in Phase I and new density just calculated. To complete the time cycle, the pressure is calculated from the density and specific internal energy and this present the starting condition for the next cycle. To help clear understanding of this calculational cycle, flow diagrams for two-dimensional case are shown in Fig. 4(a) and (b). FORTRAN program for the present calculation is listed in appendix.

5. RESULTS AND DISCUSSIONS

Using the numerical technique described in the prior section, four cases for cylindrical shock tube and one for two-dimensional were calculated for various combinations of diaphragm opening times and diaphragm pressure ratios. These cases with some representative results are summarized in Table 1. Both driver and driven gases were assumed to be ideal gases and the value of specific heat ratio, γ was taken to be 1.4. The hydraulic diameter of the shock tube, D was assumed to be 10 cm. All numerical calculations were performed on HITAC 5020 Fs at Institute of Space and Aeronautical Science, University of Tokyo and National Aerospace Laboratory.

TABLE 1. Summary of calculational conditions and results.

| P_{41} | MEMSTP | N | CPUT | τ_{op} (μ sec) | X_f/D | M_s |
|----------|--------|------|------|-----------------------------|---------|-------|
| 100 | 6 | 480 | 1801 | 99.3 | 7.8 | 2.40 |
| | 16 | 520 | 1801 | 264.7 | 8.2 | 2.40 |
| | 16 | " | " | " | 8.6 | 2.39 |
| | 30 | 600 | 1963 | 496.3 | >10.7 | >2.36 |
| 1000 | 16 | 1200 | 5119 | 264.7 | 12.0 | 3.30 |

Shock formation process

Henshall [16] has explained the process of shock formation as follows; when the bowed diaphragm is ruptured, a number of curved compression waves are propagated into the channel. These compression waves very quickly coalesce to form a curved shock wave. Its profile will become less curved as it progresses down the channel. Regular reflection of this curved shock will take place at the walls of the tube until the angle of incidence of the shock is such that regular reflection of the shock is impossible and the shock then undergoes Mach reflection. The triple points of the Mach reflection move toward the center of the tube, thus producing a plane shock wave. Subsequently, the triple points continue to move back and forth across the tube until the secondary branches of the Mach configuration are very weak and disappear. Finally, an optically flat primary shock is propagated down the channel.

Experimental investigations on the process of shock formation after diaphragm rupture have been performed by Geiger and Mautz [17] for the Cellophane diaphragms in a 2"×7" shock tube using the Shadowgraph technique. Ikui and Matsuo [18] have also investigated the process in a 38×38 mm shock tube by the Schlieren method. Photographs obtained by Geiger and Mautz support Henshall's explanation.

To see the flow patterns near the diaphragm at the initial stage of the opening process, calculated velocity distributions near the diaphragm are shown in Fig. 5 (a)–(c) for the case of $\tau_{op}=496.3 \mu\text{sec}$ and locations of shock fronts at various radial positions are also displayed in Fig. 6(a)–(c). Fig. 6(a) shows the result for diaphragm pressure ratio, $P_{41}=100$ and $\tau_{op}=264.7 \mu\text{sec}$, 6(b) is for the same diaphragm pressure ratio as 6(a) but $\tau_{op}=496.3 \mu\text{sec}$. Result for $P_{41}=1000$ and $\tau_{op}=264.7 \mu\text{sec}$ is plotted in Fig. 6(c).

The followings can be seen from Figs. 5 and 6; immediately after the diaphragm rupture, radial flow of the high pressure gas is initiated and a weak curved shock first formed by coalescence of compression waves becomes gradually plane as it propagates down the tube, which shows that the one-dimensional assumption does

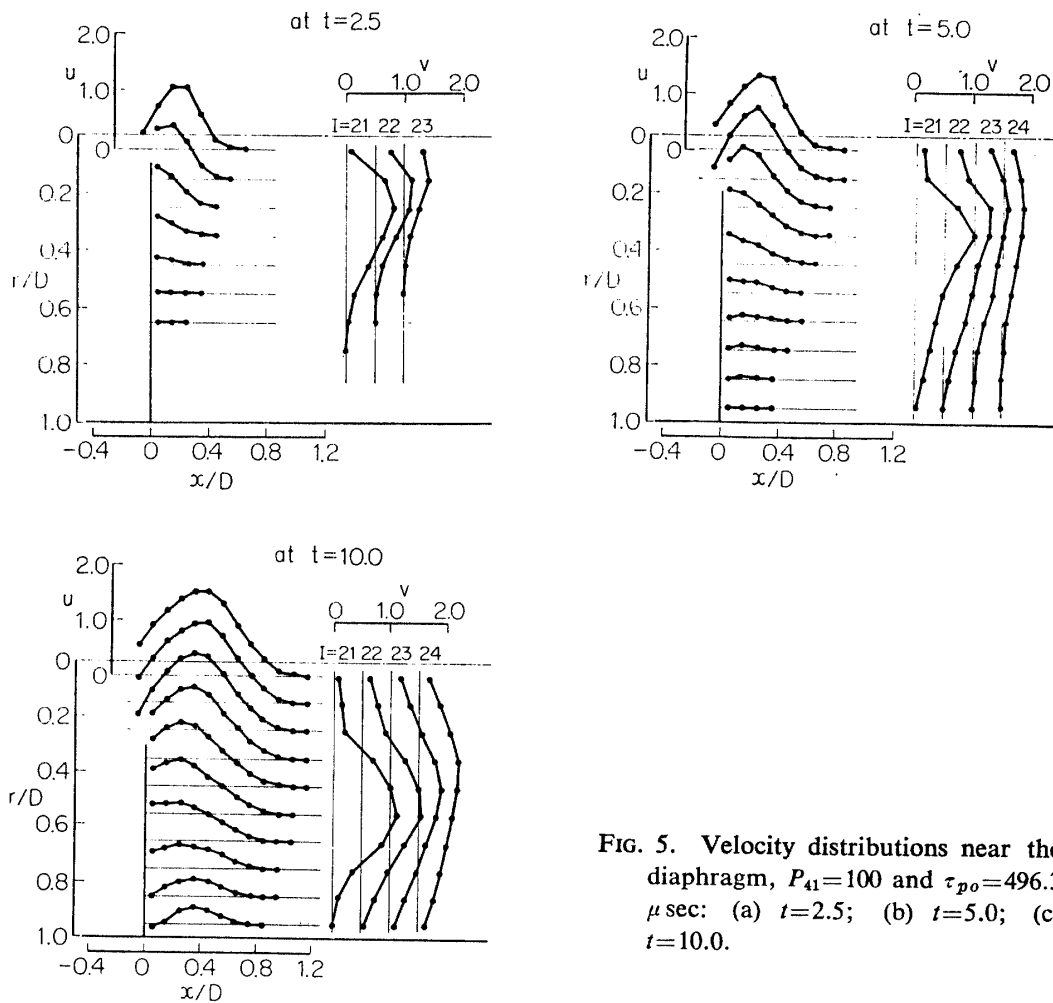


FIG. 5. Velocity distributions near the diaphragm, $P_{41}=100$ and $\tau_{po}=496.3 \mu\text{sec}$: (a) $t=2.5$; (b) $t=5.0$; (c) $t=10.0$.

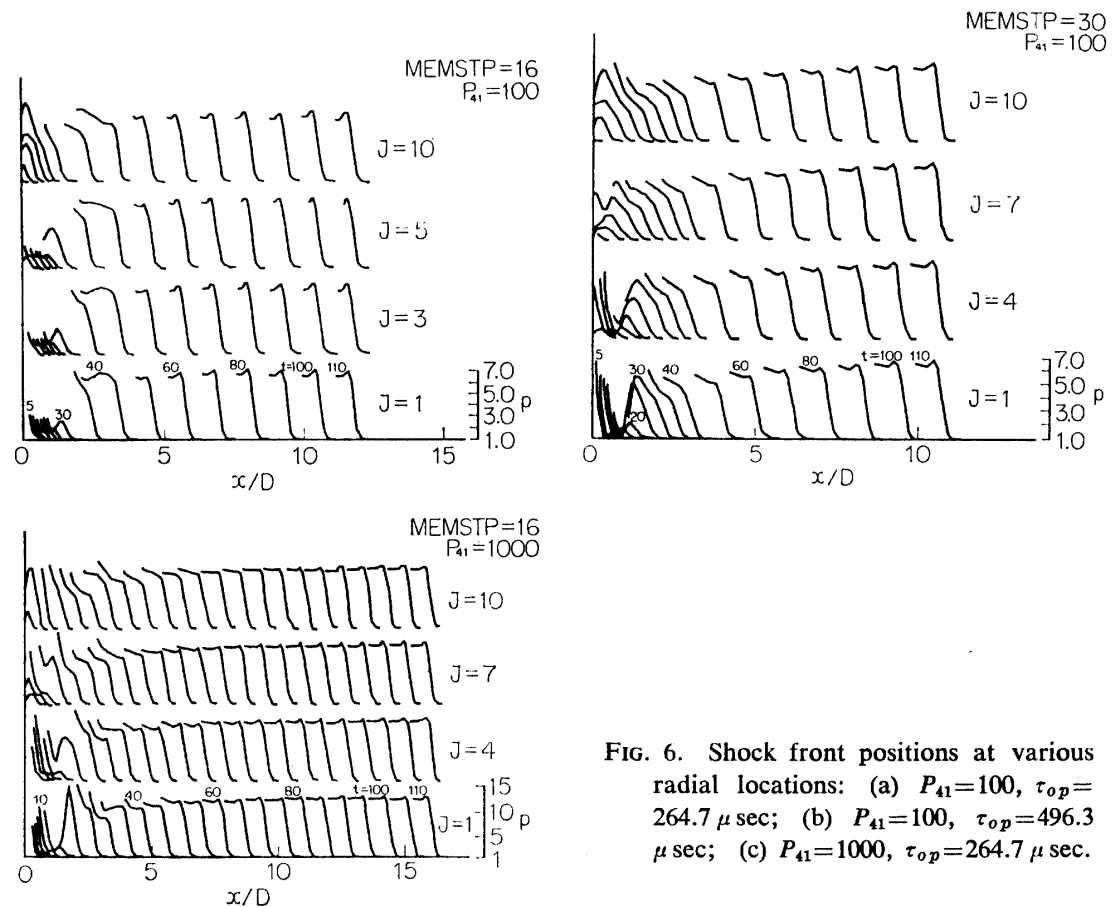


FIG. 6. Shock front positions at various radial locations: (a) $P_{41}=100$, $\tau_{op}=264.7 \mu \text{sec}$; (b) $P_{41}=100$, $\tau_{op}=496.3 \mu \text{sec}$; (c) $P_{41}=1000$, $\tau_{op}=264.7 \mu \text{sec}$.

not hold in this case. Distance travelled by the primary shock before it becomes plane is about 2 to 3 diameters. This result agrees well with that of 2.4 times hydraulic diameters obtained by above-mentioned experiment of Ikui and Matsuo. Results presented in Figs. 5 and 6 seem to support Henshall's explanation. Although, transition from regular reflection to Mach one cannot be fully identified due to insufficient resolution. Photographic investigation of Geiger and Mautz also proves this process as was indicated before. On the other hand, Ikui and Matsuo report that such reflected waves cannot be observed in their experiment but it should be considered that sensitivity of the Schlieren apparatus was not satisfactory.

Shock formation distance

As is generally known, shock formation distance is one of the most important parameters in the shock tube problems but it is very difficult to determine this theoretically. In this section we shall discuss the effect of the diaphragm opening time on shock formation distance. Fig. 7 shows $x-t$ diagrams calculated by FLIC method for various combinations of diaphragm pressure ratio, P_{41} and diaphragm opening time, τ_{op} . In Fig. 7 $x-t$ diagrams predicted by the ideal shock tube theory are also shown. Since the slope of tangent of $x-t$ diagram is reciprocal of shock speed, the smaller incrementation shows the higher shock Mach number. As is

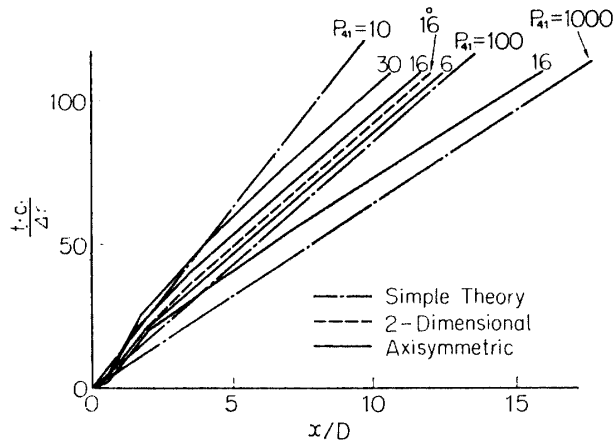


FIG. 7. Calculated $x-t$ diagram for $j=1$ cells.

clearly seen from Fig. 7 the shock front is accelerated by succeeding compression waves gradually to its final speed. This seems to prove that multi stage model proposed by Ikui and Matsuo is reasonable. Although shock formation distances tend to increase with diaphragm opening time, for the same diaphragm pressure ratio shock Mach numbers converge to a value which is greater than that predicted by ideal shock tube theory. As in our model of diaphragm opening process applied to this calculation, rate of change of cross-sectional area opened to high pressure gas is set to be proportional to time in two-dimensional case and to square of time in cylindrical case for the convenience of calculation, for the same diaphragm opening time, shock front is accelerated faster in two-dimensional case than in cylindrical case, which can be clearly seen in Fig. 7.

From $x-t$ diagrams displayed in Fig. 7 variations of shock Mach numbers along the shock tube axis are obtained and plotted in Fig. 8 for several diaphragm opening time for the case of $P_{41}=100$. Fig. 8 also shows the tendency that although acceleration of shock fronts is slower for larger diaphragm opening time, shock Mach numbers for all cases converge to the same value. This shows a qualitative agreement with the result of Shtemenko's experiment [19]. In his experiment,

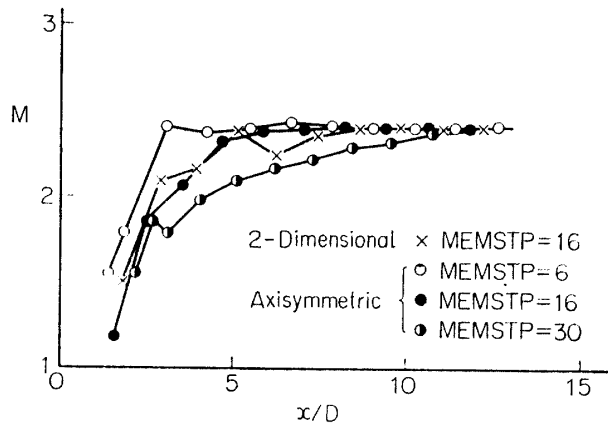


FIG. 8. Variation of shock Mach numbers with distance along shock tube axis.

maximum shock Mach numbers decrease slightly with increasing diaphragm opening time but this may be due to the effect of viscosity and should be a constant value neglecting such effect. As is clearly seen from Figs. 7 and 8, for the case of $\tau_{op} = 496.3 \mu\text{sec}$, the largest value of diaphragm opening time, shock front is still accelerating. Shock formation distances calculated from Fig. 8 are tabulated in Table 1.

Shock tube performance

According to the ideal shock tube theory, shock Mach numbers are easily calculated from specific heat ratios of driver and driven gases, diaphragm pressure ratio and initial temperature ratio. In actual shock tubes, however, shocks with higher Mach numbers than predicted by the ideal theory have been observed for diaphragm pressure ratios of the order of 10^4 . Ikui and Matsuo [18] have reported that even for the diaphragm pressure ratios less than 10^2 , stronger shocks than predicted by ideal theory were observed in a shock tube with large diameter. The formation-from-compression model proposed by White predicts significantly stronger shock waves than the usual ideal model for the larger diaphragm pressure ratios. Multi stage model proposed by Ikui and Matsuo which is an extension of White's model to take into account the effects of shock acceleration gives still stronger shocks than White's model.

In the present calculation by FLIC numerical method we did not base upon the one-dimensional assumption on which all the above-mentioned models were based. In Fig. 9 calculated shock tube performance is plotted and compared with those predicted by ideal, White's and multi stage model. Present result shows a close agreement with multi stage model for the cases of $P_{41} = 10$ and 100 but significantly higher shock Mach number is predicted for $P_{41} = 1000$. Calculated data are so insufficient to draw any conclusion about this that further investigations should be needed.

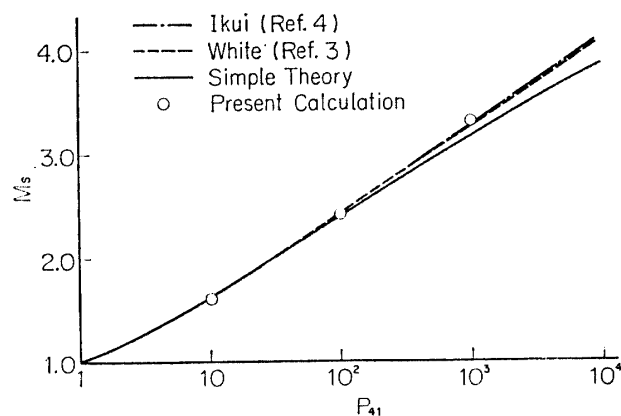


FIG. 9. Predicted shock tube performance for air/air.

6. CONCLUDING REMARKS

It may be summarised from the calculated result using the FLIC method that shock formation process is not one-dimensional as assumed in ideal shock tube theory and other models proposed by various authors, and shock formation distances tend to increase with diaphragm opening time and with diaphragm pressure ratios, which shows qualitative agreement with experimental results. For $P_{41}=100$, calculated shock formation distances varies from about 8 diameters to above 11 according to the diaphragm opening time. For $\tau_{op}=496.3 \mu\text{sec}$, the largest value of diaphragm opening time shock front is still accelerating. Calculated shock tube performance shows a close agreement with that predicted by multi stage model for the cases of $P_{41}=10$ and 100. For $P_{41}=1000$, however, significantly higher shock Mach number is predicted by FLIC method. Calculated data are so insufficient to draw any conclusion that further investigation should be needed.

ACKNOWLEDGEMENT

The author would like to express his gratitude to Prof. Ryuma Kawamura of Institute of Space and Aeronautical Science, University of Tokyo for his continuous guidance and helpful discussion. The author is also greatly indebted to Dr. Takayuki Aki of National Aerospace Laboratory for making computer time available for this study and to Mr. Naoki Hirose for the considerable assistance with the computer programming.

*Department of Aerodynamics
Institute of Space and Aeronautical Science,
University of Tokyo, Tokyo
April 20, 1970*

REFERENCES

- [1] Glass, I. I. and Patterson, G. N.: A Theoretical and Experimental Study of Shock-Tube Flows, *J. Aero. Sci.* 22, 73-100 (1955).
- [2] Glass, I. I.: Shock Tubes. Part I: Theory and Performance of Simple Shock Tubes, Institute of Aerophysics, University of Toronto, UTIA Review No. 12, Part I (1958).
- [3] White, D. R.: Influence of Diaphragm Opening Time on Shock-Tube Flows, *J. Fluid Mech.* 4, 585-599 (1958).
- [4] Ikui, T., Matsuo, K. and Nagai, M.: A Study on Aerodynamic Characteristics of Shock Tubes. Part 2: Shock Formation Process (in Japanese), *Trans. JSME*, 34, 1969-1976 (1968).
- [5] Gentry, R. A., Martin, R. E. and Daly, B. J.: An Eulerian Differencing Method for Unsteady Compressible Flow Problems, *J. Comp. Phys.* 1, 87-118 (1966).
- [6] Campbell, G. A., Kimber, G. M. and Napier, D. J.: Bursting of Diaphragms as related to the Operation of Shock Tubes, *J. Sci. Instrum.* 42, 381-384 (1965).
- [7] Lax, P. D.: Weak Solutions of Nonlinear Hyperbolic Equations and Their Numerical Computation, *Comm. Pure Appl. Math.*, 7, 159-193 (1954).
- [8] Godunov, S. K.: A Finite Difference Method for the Numerical Computation and

- Discontinuous Solution of the Equation of Fluid Dynamics, *Math. Sbornik*, **47**, 271 (1959).
- [9] Rusanov, V. V.: The Calculation of the Interaction of Non-Stationary Shock Waves and Obstacles, *Zhur. Vychis. Fiziki*, **1**, 267-279 (1961).
 - [10] Lax, P. D. and Wendroff, B.: Systems of Conservation Laws, *Comm. Pure Appl. Math.*, **13**, 271-237 (1960).
 - [11] Evans, M. W. and Harlow, F. H.: The Particle-in-Cell Method for Hydrodynamic Calculations, Los Alamos Scientific Lab. Rept. LA-2139 (1957).
 - [12] Harlow, F. H.: Hydrodynamic Problems Involving Large Fluid Distortion, *J. Assoc. Comp. Mech.*, **4**, 137 (1957).
 - [13] Amsden, A. A.: The Particle-in-Cell Method for the Calculation of the Dynamics of Compressible Fluids, Los Alamos Scientific Lab. Rept. LA-3466 (1966).
 - [14] Emery, A. F.: An Evaluation of Several Differencing Methods for Inviscid Fluid Flow Problems, *J. Comp. Phys.*, **2**, 306-331 (1968).
 - [15] Rich, M.: A Method for Eulerian Fluid Dynamics, Los Alamos Scientific Lab. Rept. LAMS-2826 (1962).
 - [16] Henshall, B. D.: On Some Aspects of the Use of Shock Tubes in Aerodynamic Research, A.R.C. Technical Rept. R. & M. No. 3044 (1957).
 - [17] Geiger, F. W. and Mautz, C. W.: The Shock Tube as an Instrument for Investigation of Transonic and Supersonic Flow Patterns, U. S. Navy Department Office at Naval Research, Project M 720-4 (1949).
 - [18] Ikui, T. and Matsuo, K.: A Study on Aerodynamic Characteristics of Shock Tubes. Part 1: Effects of Tube Diameter on Performance (in Japanese), *Trans. JSME*, **34**, 1961-1968 (1968).
 - [19] Shtemenko, P. S.: *Bestnik Moskovskobo Unibersiteta*, **22**, 58 (1967).

APPENDIX

| | | | |
|-------|--|-----|-----|
| C *** | *** | | |
| C | COMMENT | | |
| C *** | *** | C | 1 |
| C *** | *** | | |
| C | HITACHI CORD | | |
| C | FLIC2C | C | 2 |
| C | NUMERICAL CALCULATION FOR AERODYNAMICS | C | 3 |
| C | FLUID-IN-CELL (FLIC) CALCULATION | C | 6 |
| C | TWO-DIMENSIONAL FORMULATION IN RECTANGULAR AND CYLINDRICAL COORDINATES | C | 7 |
| C | TWO-DIMENSIONAL SHOCK FORMATION IN A SHOCK TUBE | C | 8 |
| C | ITYPE = 1 RECTANGULAR COORDINATES | C | 9 |
| C | ITYPE = 2 CYLINDRICAL COORDINATES | | |
| C | ITAPE = 1 I/O EXECUTION | | |
| C | ITAPE = 0 I/O NON EXECUTION | | |
| C | COMPUTATION TIME SAVING PROGRAMME | | |
| C | ISTP(J).....CALCULATION FROM I=1 TO ISTP(J) | C | |
| C | PRINT PAGE SAVING PROGRAMME | | |
| C | ISTPP(J).....PRINT FROM I=1, TO ISTPP(J) | C | |
| C *** | *** | | |
| C *** | *** | | |
| C | INITIAL SET-UP | SUP | 1 |
| C *** | *** | | |
| C *** | *** | | |
| | DIMENSION RGU(440,10),P(440,10),C(440,10),U(440,10),V(440,10),UTD(| SUP | 2H |
| | 1440,10),VTD(440,10),EI(440,10),ETD(440,10),E(440,10),ETD(440,10), | SUP | 3H |
| | 2QUL(440),DQUL(440),ISTP(10),ISTPP(10) | SUP | 4H |
| | EQUIVALENCE (P,E) | SUP | 5 |
| | CALL DPOH | SUP | 6 |
| | CALL OPGOP(3) | SUP | 61 |
| 70 | WRITE(6,1) | SUP | 7 |
| 60 | READ(5,2)DX,DR,GAM,STEP | SUP | 8 |
| | IF(DX.EQ.0.) GO TO 70 | SUP | 9 |
| | IF(DX.LT.0.) STOP | SUP | 10 |
| | READ(5,3)UINF,PINF,CINF,RATIO | SUP | 11 |
| | READ(5,4)IN1,IN2,IN3,IN,ITYPE | SUP | 12 |
| | READ(5,5)LJ1,LJ2,LJ3,NPR1,NPR2,ILAST,ISTART,IRUN | SUP | 13 |
| | READ(5,6)JAK,B | SUP | 14 |
| | READ(5,7)ITAPE | SUP | 14A |
| | IF(ITAPE.EQ.1) REWIND 3 | SUP | 14B |
| 1 | FORMAT(1H1,30RFLUID IN CELL CALCULATION | SUP | 15 |
| 2 | FORMAT(4F12.0) | SUP | 16 |
| 3 | FORMAT(5F12.0) | SUP | 17 |
| 4 | FORMAT(4I8) | SUP | 18 |
| 5 | FORMAT(8I8) | SUP | 19 |
| 6 | FORMAT(2F12.0) | SUP | 20 |
| 7 | FORMAT(18) | SUP | 201 |
| | READ(5,50)MEMSTP,IMT | SUP | 21 |
| 50 | FORMAT(2I8) | SUP | 22 |
| | PAI=3.14159 | SUP | 23 |
| | ROINF=GAM*PINF/CINF**2 | SUP | 24 |
| | EINF=PINF/((GAM-1.)*ROINF) | SUP | 25 |
| | BINF=BINF+(UINF**2+VINF**2)/2. | SUP | 26 |
| | IN=IN1+IN2 | SUP | 27 |
| | T=0. | SUP | 28 |
| | ITIME=0 | SUP | 29 |
| | ITOPP=0 | SUP | 29A |
| | IPRINT=LJ1 | SUP | 30 |

| | | | |
|-------|--|------|-----|
| | MEMR=0 | SUP | 31 |
| | DT=STEP*DX/CINF | SUP | 32 |
| | IF(DR.LE.DX) DT=STEP*DR/CINF | SUP | 33 |
| | DO 8 J=1,JN | SUP | 34 |
| | DO 9 I=1,IN | SUP | 35 |
| | ROU(I,J)=ROINF | SUP | 36 |
| | IF(I.LE.IN1) ROU(I,J) =RATIO*ROINF | SUP | 37 |
| | EI(I,J)=EIINF | SUP | 38 |
| | U(I,J)= UINF | SUP | 39 |
| | V(I,J)= VINF | SUP | 40 |
| 9 | CONTINUE | SUP | 41 |
| 8 | CONTINUE | SUP | 42 |
| | CMTOT=0. | SUP | 43 |
| | ETOT=0. | SUP | 44 |
| | VOL=DX*DR | SUP | 45 |
| | DO 10 J=1,JN | SUP | 46 |
| | IF(ITYPE.EQ.2) VOL=2. *PAI*(FLOAT(J)-0.5)*DX*DR**2 | SUP | 47 |
| | DO 11 I=1,IN | SUP | 48 |
| | CMTOT=CMTOT+ROU(I,J)*VOL | SUP | 49 |
| | E(I,J)=EI(I,J)+(U(I,J)**2+V(I,J)**2)/2. | SUP | 50 |
| | ETOT=ETOT+E(I,J)*ROU(I,J)*VOL | SUP | 51 |
| 11 | CONTINUE | SUP | 52 |
| 10 | CONTINUE | SUP | 53 |
| | ETH=ETOT | SUP | 54 |
| | CMTH=CMTOT | SUP | 55 |
| | EPSE=10.0*EINF/ETOT | SUP | 56 |
| | EPSE=1. E-3 | SUP | 57 |
| | IF(IRUN.GE.2) GO TO 888 | SUP | 58 |
| | WRITE(6,14) | SUP | 59 |
| 14 | FORN=1,4,ACHINITIAL TIME FLOW FIELD PROPERTY PLOT) | SUP | 60 |
| | DO 12 J=1,JN | SUP | 61M |
| | ISTP(J)=IN1+1 | SUP | 62M |
| | ISTPP(J)=IN1+1 | SUP | 62M |
| 12 | CONTINUE | SUP | 63M |
| | GO TO 605 | SUP | 64M |
| C *** | *** | | |
| C *** | *** | | |
| C | I-1 PRESSURE AND SOUND SPEED CALCULATION | I -1 | 1 |
| C *** | *** | | |
| C *** | *** | | |
| 888 | READ(3) ITIME, IPRINT, CMTH, ETH,DT | I -1 | 1 |
| | READ(3) ((ROU(I,J),U(I,J),V(I,J),EI(I,J),I=1,IN),J=1,JN) | I -1 | 2 |
| | IF(ITIME.EQ.ISTART) GO TO 102 | I -1 | 3 |
| | GO TO 888 | I -1 | 4 |
| 102 | DO 103 J=1,JN | I -1 | 6 |
| | DO 104 I=1,IN | I -1 | 7 |
| | P(I,J)=(GAM-1.)*ROU(I,J)*EI(I,J) | I -1 | 8 |
| | C(I,J)=S*RT(GAM*(GAM-1.)*EI(I,J)) | I -1 | 9 |
| 104 | CONTINUE | I -1 | 10 |
| 103 | CONTINUE | I -1 | 11 |
| | IF(ITIME.EQ.ISTART) GO TO 118 | I -1 | 11A |
| | IF(ROD(IPRIME,IPRINT).EQ.0) GO TO 105 | I -1 | 12 |
| | GO TO 118 | I -1 | 13 |
| 105 | DO 106 J=1,JN | I -1 | 14 |
| | WRITE(6,108) J | I -1 | 15 |
| | WRITE(6,109) | I -1 | 16 |
| | ISTP1=ISTP(J) | I -1 | 161 |

```

DO 107 I=1,INTPP1
ABVEL=SQRT(U(I,J)**2+V(I,J)**2)
AMACH=ABVEL/C(I,J)
SPEED=ABVEL/SINF
IF (ABVEL.EQ.0.) GO TO 151
IF(U(I,J)**2.LE.V(I,J)**2) GO TO 150
ANGLE=ATAN(V(I,J)/U(I,J))*57.29578
IF(U(I,J).LT.0. .AND.V(I,J).GE.0.) ANGLE=ANGLE+180
IF(U(I,J).LT.0. .AND.V(I,J).LT.0.) ANGLE=ANGLE-180
GO TO 152
150 IF(V(I,J).GE.0.) GO TO 149
ANGLE=-90. -ATAN(U(I,J)/V(I,J))*57.29578
GO TO 152
149 ANGLE=90. - ATAN(U(I,J)/V(I,J))*57.29578
GO TO 152
151 ANGLE=0.
152 NMOD=MOD(I,3)+1
GO TO (111,109,110),NMOD
109 WRITE(6,113)I, P(I,J),AMACH,SPEED,ANGLE
GO TO 107
110 WRITE(6,114)I, P(I,J),AMACH,SPEED,ANGLE
GO TO 107
111 WRITE(6,115)I, P(I,J),AMACH,SPEED,ANGLE
107 CONTINUE
108 CONTINUE
999) FORMAT(1H0,3(40H I PRESSURE AMACH SPEED ANGLE ))
108 FORMAT(1H0,2HJ=I5)
113 FORMAT(1H , 14,4F9.4 )
114 FORMAT(1H+,40X, 14,4F9.4)
115 FORMAT(1H+,50X, 14,4F9.4)
118 IF(ITIME.EQ.ILAST) GO TO 119
IF(P(IN,1).GE.1.5*PINF) GO TO 119
ITIME=ITIME+1
IF(ITIME.GE.NPR1.AND.ITIME.LT.NPR2) IPRINT=LJ2
IF(ITIME.GE.NPR2) IPRINT=LJ3
IF(MOD(ITIME,MEMSTEP).EQ.1) MEMR=MEMR+1
IF(MEMR.GE.JN) MEMR=JN
IF(ITIME.NE.IDT) GO TO 199
ITOFF=IDT-1
DT=2.0*DT
TOPF=T
GO TO 199
119 IF(ITAPE.NE.1) GO TO 60
REWIND 3
GO TO 60
C *** ***
C *** ***
C I-2 THE PILE VELOCITY CALCULATION I -2 1
C *** ***
C *** ***
199 VOL=DX*DR I -2 2
S2=DX I -2 3
S4=DX I -2 4
J=1 I -2 5
200 IF(ITYPE.NE.2) GO TO 201 I -2 6
VOL=2. *PAI*(FLOAT(J)-.5)*DX*DR**2 I -2 7
S2=2. *PAI*FLOAT(J-1)*DR*DX I -2 8

```

| | | | |
|-----|---|------|-----|
| | S4=2. *PAI*FLOAT(J)*DR*DX | I -2 | 9 |
| 201 | I=1 | I -2 | 10 |
| 202 | IF(I.EQ.1.OR.(I.EQ.IN1+1.AND.J.GT.MEMR)) GO TO 203 | I -2 | 11 |
| | P1=P(I-1,J) | I -2 | 12 |
| | Q1=QRL | I -2 | 13 |
| | GO TO 204 | I -2 | 14 |
| 203 | P1=P(I,J) | I -2 | 15 |
| | Q1=0. | I -2 | 16 |
| | IF((AK*(U(I,J)**2+V(I,J)**2).LT.C(I,J)**2).AND.(U(I,J).LT.O.)) | I -2 | 17 |
| | 1 Q1=-2. *B*C(I,J)*U(I,J)*ROU(I,J) | I -2 | 18 |
| 204 | IF(J.EQ.1) GO TO 205 | I -2 | 19 |
| | P2=P(I,J-1) | I -2 | 20 |
| | Q2=QUL(I) | I -2 | 21 |
| | GO TO 206 | I -2 | 22 |
| 205 | P2=P(I,J) | I -2 | 23 |
| | Q2=0. | I -2 | 24 |
| | IF((TYPE.EQ.1).AND.(AK*(U(I,J)**2+V(I,J)**2).LT.C(I,J)**2).AND.(V(I | I -2 | 25 |
| | 1(I,J).LT.O.)) Q2=-2. *B*C(I,J)*ROU(I,J)*V(I,J) | I -2 | 26 |
| 206 | IF(I.EQ.IN.OR.(I.EQ.IN1.AND.J.GT.MEMR)) GO TO 207 | I -2 | 27 |
| | P3=P(I+1,J) | I -2 | 28 |
| | Q3=0. | I -2 | 29 |
| | IF((AK*(U(I,J)**2+U(I+1,J)**2+V(I,J)**2+V(I+1,J)**2).LT.(C(I,J)**2I | I -2 | 30 |
| | 1+C(I+1,J)**2)).AND.(U(I,J).GT.U(I+1,J))) Q3=B*(C(I,J)+C(I+1,J))* | I -2 | 31 |
| | 2(ROU(I,J)+ROU(I+1,J))*(U(I,J)-U(I+1,J))/4. | I -2 | 32 |
| | QRL=Q3 | I -2 | 33 |
| | GO TO 208 | I -2 | 34 |
| 207 | P3=P(I,J) | I -2 | 35 |
| | Q3=0. | I -2 | 36 |
| | IF((AK*(U(I,J)**2+V(I,J)**2).LT.C(I,J)**2).AND.(U(I,J).GT.O.)) | I -2 | 37 |
| | 1 Q3=2. *B*C(I,J)*ROU(I,J)*U(I,J) | I -2 | 38 |
| 208 | IF(J.EQ.JN) GO TO 209 | I -2 | 39 |
| | P4=P(I,J+1) | I -2 | 40 |
| | Q4=0. | I -2 | 41 |
| | IF((AK*(U(I,J)**2+U(I,J+1)**2+V(I,J)**2+V(I,J+1)**2).LT.(C(I,J)**2I | I -2 | 42 |
| | 1+C(I,J+1)**2)).AND.(V(I,J).GT.V(I,J+1))) Q4=B*(C(I,J)+C(I,J+1))* | I -2 | 43 |
| | 2(ROU(I,J)+ROU(I,J+1))*(V(I,J)-V(I,J+1))/4. | I -2 | 44 |
| | QUL(I)=Q4 | I -2 | 45 |
| | GO TO 210 | I -2 | 46 |
| 209 | P4=P(I,J) | I -2 | 47 |
| | Q4=0. | I -2 | 48 |
| | IF((AK*(U(I,J)**2+V(I,J)**2).LT.C(I,J)**2).AND.(V(I,J).GT.O.))Q4=1 | I -2 | 49 |
| | 1 2. *B*C(I,J)*ROU(I,J)*V(I,J) | I -2 | 50 |
| 210 | UTD(I,J)=U(I,J)-DT*(.5*(P3-P1)+Q3-Q1)/(ROU(I,J)*LX) | I -2 | 51 |
| | VTD(I,J)=V(I,J)-DT*((S4*(P4-P(I,J))-S2*(P2-P(I,J)))/(2.*VOL)+(Q4 | I -2 | 52 |
| | 1 -Q2)/DR)/ROU(I,J) | I -2 | 53 |
| | IF((UTD(I,J).GE.DX/DT).OR.(VTD(I,J).GE.DR/DT)) GO TO 213 | I -2 | 54 |
| | IF((UTD(I,J)**2+VTD(I,J)**2.LE.O.O).AND.(I.J).LE.ROINF)) GO | I -2 | 55M |
| | 1 TO 250 | I -2 | 56M |
| | IF(I.GE.IN) GO TO 251 | I -2 | 57M |
| 211 | I=I+1 | I -2 | 58M |
| | GO TO 202 | I -2 | 59M |
| 250 | ISTP(J)=I+3 | I -2 | 60M |
| | GO TO 252 | I -2 | 61M |
| 251 | ISTP(J)=I | I -2 | 62M |
| 252 | IF(J.GE.JN) GO TO 300 | I -2 | 63M |
| | J=J+1 | I -2 | 64M |
| | GO TO 200 | I -2 | 65M |

```

213 DT=DT/2 I -2 61
WRITE(6,6666)DT,ITIME I -2 62
6666 FORMAT(1H0,22H TIME STEP IS TOO LARGE //1H ,18H NEW TIME STEP DT= I -2 63
1 F12.6,18H AT TIME CYCLE NO.= I8) I -2 64
GO TO 199 I -2 65
C *** ***
C *** ***
C I-3 THE TILDE INTERNAL ENERGY CALCULATION I -3 1
C *** ***
C *** ***
300 VOL=DX*DR I -3 2
S1=DR I -3 3
S2=DX I -3 4
S4=DX I -3 5
S2H4=DX I -3 6
S4PH=DX I -3 7
S2MH=DX I -3 8
J=1 I -3 9
301 IF(ITYPE.NE.2) GO TO 302 I -3 10
FJ=J I -3 11
VOL=2. *PAI*(FJ - .5)*DX*DR**2 I -3 12
S1=2. *PAI*(FJ- .5)*DR**2 I -3 13
S2=2. *PAI*(FJ-1. )*DR*DX I -3 14
S4=2. *PAI*FJ*DR*DX I -3 15
S2H4=2. *PAI*(FJ- .5)*DR*DX I -3 16
S4PH=2. *PAI*(FJ+ .5)*DR*DX I -3 17
S2MH=0. I -3 18
IF(J.GT.1) S2MH=2. *PAI*(FJ-1.5)*DR*DX I -3 19
302 I=1 I -3 20
303 IF(I.EQ.1.OR.(I.EQ.IN1+1.AND.J.GT.MEMM)) GO TO 304 I -3 21
U1=U(I-1,J)+UTD(I-1,J) I -3 22
Q1=QRL I -3 23
GO TO 305 I -3 24
304 U1=-(U(I,J)+UTD(I,J)) I -3 25
Q1=0. I -3 26
IF((AK*(U(I,J)**2+V(I,J)**2).LT.C(I,J)**2).AND.(U(I,J).LT.O. )) I -3 27
1 Q1=-2. *B*C(I,J)*ROU(I,J)*U(I,J) I -3 28
305 IF(J.EQ.1) GO TO 306 I -3 29
V2=V(I,J-1)+VTD(I,J-1) I -3 30
Q2=QUL(I) I -3 31
GO TO 307 I -3 32
306 V2=-(V(I,J)+VTD(I,J)) I -3 33
Q2=0. I -3 34
IF((ITYPE.EQ.1).AND.(AK*(U(I,J)**2+V(I,J)**2).LT.C(I,J)**2).AND.(V I -3 35
1(I,J).LT.O. )) Q2=-2. *B*C(I,J)*ROU(I,J)*V(I,J) I -3 36
307 IF(I.EQ.IN.OR.(I.EQ.IN1.AND.J.GT.MEMR)) GO TO 308 I -3 37
U3=U(I+1,J)+UTD(I+1,J) I -3 38
Q3=0. I -3 39
IF((AK*(U(I,J)**2+U(I+1,J)**2+V(I,J)**2+V(I+1,J)**2).LT.(C(I,J)**2 I -3 40
1+C(I+1,J)**2)).AND.(U(I,J).GT.U(I+1,J))) Q3=B*(C(I,J)+C(I+1,J))* I -3 41
2(ROU(I,J)+ROU(I+1,J))*(U(I,J)-U(I+1,J))/4. I -3 42
QRL=Q3 I -3 43
GO TO 309 I -3 44
308 IF(I.EQ.IN) GO TO 350 I -3 45
U3=-(U(I,J)+UTD(I,J)) I -3 45
Q3=0. I -3 46
IF((AK*(U(I,J)**2+V(I,J)**2).LT.C(I,J)**2).AND.(U(I,J).GT.O. )) I -3 47

```

```

1Q3=2. *B*C(I,J)*ROU(I,J)*U(I,J) I -3 48
GO TO 309 I -3 481
350 U3= U(I,J)+UTD(I,J) I -3 482
Q3= 0. I -3 483
309 IF(J.EQ.JN) GO TO 310 I -3 49
V4=V(I,J+1)+VTD(I,J+1) I -3 50
Q4=0. I -3 51
IF((AK*(U(I,J)**2+U(I,J+1)**2+V(I,J)**2+V(I,J+1)**2).LT.(C(I,J)**2 I -3 52
1+C(I,J+1)**2)).AND.(V(I,J).GT.V(I,J+1))) Q4=B*(C(I,J)+C(I,J+1))* I -3 53
2 (ROU(I,J)+ROU(I,J+1))*(V(I,J)-V(I,J+1))/4. I -3 54
Q4(I)=Q4 I -3 55
GO TO 311 I -3 56
310 V4=- (V(I,J)+VTD(I,J)) I -3 57
Q4=0. I -3 58
IF((AK*(U(I,J)**2+V(I,J)**2).LT.C(I,J)**2).AND.(V(I,J).GT.O. ))Q4=I -3 59
1 2. *B*C(I,J)*ROU(I,J)*V(I,J) I -3 60
311 UTEMP=U(I,J)+UTD(I,J) I -3 61
VTEMP=V(I,J)+VTD(I,J) I -3 62
E1TD(I,J)=E1(I,J)-DT*(P(I,J)*(S4*(V4+VTEMP)-S2* (V2+VTEMP))/4. I -3 63
1 +(Q3*(SAPH*V4+S2H4*VTEMP)-Q2*(S2H4*VTEMP+S2MH*V2))/4. I -3 64
2 -(VTEMP*S2H4*(Q4-Q2)+UTEMP*S1*(Q3-Q1))/2. I -3 65
3 +S1*(UTEMP+U3)*(P(I,J)+Q3)-(UTEMP+U1)*(P(I,J)+Q1))/4. ) I -3 66
4 /(ROU(I,J)*VOL) I -3 67
ETD(I,J)=E1TD(I,J)+(UTD(I,J)**2+VTD(I,J)**2)/2. I -3 68
IF(I.GE.ISTP(J)) GO TO 312 I -3 69
I=I+1 I -3 70
GO TO 303 I -3 71
312 IF(J.EQ.JN) GO TO 400 I -3 72
J=J+1 I -3 73
GO TO 301 I -3 74
C *** ***
C *** ***
C II-1 CALCULATION OF TRANSPORT EFFECTS II -1 1
C *** ***
C *** ***
400 VOL=DX*DR II-1 2
S1=DR II-1 3
S2=DX II-1 4
S4=DX II-1 5
J=1 II-1 6
401 IF(ITYPE.NE.2) GO TO 402 II-1 7
FJ=J II-1 8
VOL=2. *PAI*(FJ - .5)*DX*DR**2 II-1 9
S1=2. *PAI*(FJ- .5)*DR**2 II-1 10
S2=2. *PAI*(FJ-1. )*DR*DX II-1 11
S4=2. *PAI*FJ*DR*DX II-1 12
402 I=1 II-1 13
403 IF(I.EQ.1.OR.(I.EQ.IN1+1.AND.J.GT.MEMR)) GO TO 404 II-1 14
U1=UTD(I-1,J) II-1 15
V1=VTD(I-1,J) II-1 16
E1=ETD(I-1,J) II-1 17
D1L=D1RL II-1 18
INT1=0 II-1 19
IF(INTRL.EQ.0) INT1=1 II-1 20
GO TO 405 II-1 21
404 U1=-UTD(I,J) II-1 22
V1= VTD(I,J) II-1 23

```

| | | | |
|-----|---|------|-----|
| | E1= ETD(I,J) | II-1 | 24 |
| | DM1=0. | II-1 | 25 |
| | INT1=1 | II-1 | 26 |
| 405 | IF(J.EQ.1) GO TO 406 | II-1 | 27 |
| | U2=UTD(I,J-1) | II-1 | 28 |
| | V2=VTD(I,J-1) | II-1 | 29 |
| | E2=ETD(I,J-1) | II-1 | 30 |
| | DM2=DMUL(I) | II-1 | 31 |
| | INT2=0 | II-1 | 32 |
| | IF(DM2.GE.0.) INT2=1 | II-1 | 33 |
| | GO TO 407 | II-1 | 34 |
| 406 | U2= UTD(I,J) | II-1 | 35 |
| | V2=VTD(I,J) | II-1 | 36 |
| | E2=ETD(I,J) | II-1 | 37 |
| | DM2=0. | II-1 | 38 |
| | INT2=0 | II-1 | 39 |
| 407 | IF(1.EQ.IN.OK.(I.EQ.IN1.AND.J.GT.MEMR)) GO TO 410 | II-1 | 40 |
| | U3=UTD(I+1,J) | II-1 | 41 |
| | V3=VTD(I+1,J) | II-1 | 42 |
| | E3=ETD(I+1,J) | II-1 | 43 |
| | IF(UTD(I,J)+UTD(I+1,J).LT.0.) GO TO 408 | II-1 | 44 |
| | DM3=ROU(I,J)*(UTD(I,J)+UTD(I+1,J))*S1*DT/2. | II-1 | 45 |
| | INT3=0 | II-1 | 46 |
| | GO TO 409 | II-1 | 47 |
| 408 | DM3=ROU(I+1,J)*(UTD(I,J)+UTD(I+1,J))*S1*DT/2. | II-1 | 48 |
| | INT3=1 | II-1 | 49 |
| 409 | DMR1=DM3 | II-1 | 50 |
| | INTR1=INT3 | II-1 | 51 |
| | GO TO 411 | II-1 | 52 |
| 410 | IF(I.EQ.IN) GO TO 460 | II-1 | 53 |
| | U3=-UTD(I,J) | II-1 | 531 |
| | V3= VTD(I,J) | II-1 | 54 |
| | E3= ETD(I,J) | II-1 | 55 |
| | DM3=0. | II-1 | 56 |
| | INT3=0 | II-1 | 57 |
| | GO TO 411 | II-1 | 571 |
| 460 | U3=UTD(I,J) | II-1 | 572 |
| | V3=VTD(I,J) | II-1 | 573 |
| | E3=ETD(I,J) | II-1 | 574 |
| | DM3=ROU(I,J)*UTD(I,J)*S1*DT | II-1 | 575 |
| | INT3=0 | II-1 | 576 |
| | IF(UTD(I,J).LT.0.) INT3=1 | II-1 | 577 |
| | CMTH=EMH-DM3*(EMD(I,J)+(GAM-1.) *EI(I,J)) | II-1 | 578 |
| | CMTH=CMTH-DM3 | II-1 | 579 |
| 411 | IF(J.EQ.JN) GO TO 414 | II-1 | 58 |
| | U4=UTD(I,J+1) | II-1 | 59 |
| | V4=VTD(I,J+1) | II-1 | 60 |
| | E4=ETD(I,J+1) | II-1 | 61 |
| | IF(VTD(I,J)+VTD(I,J+1).LT.0.) GO TO 412 | II-1 | 62 |
| | DM4=ROU(I,J)*(VTD(I,J)+VTD(I,J+1))*S4*DT/2. | II-1 | 63 |
| | INT4=0 | II-1 | 64 |
| | GO TO 413 | II-1 | 65 |
| 412 | DM4=ROU(I,J+1)*(VTD(I,J)+VTD(I,J+1))*S4*DT/2. | II-1 | 66 |
| | INT4=1 | II-1 | 67 |
| 413 | DMUL(I)=DM4 | II-1 | 68 |
| | GO TO 415 | II-1 | 69 |
| 414 | U4= UTD(I,J) | II-1 | 70 |

| | | | |
|-------|---|------|------|
| | V4=-VTD(I,J) | II-1 | 71 |
| | E4= ETD(I,J) | II-1 | 72 |
| | D*4=0. | II-1 | 73 |
| | INT4=0 | II-1 | 74 |
| 415 | ROUNP1=ROU(I,J)+(DM1+DM2-DM3-DM4)/VOL | II-1 | 75 |
| | AIN1=INT1 | II-1 | 76 |
| | AIN2=INT2 | II-1 | 77 |
| | AIN3=INT3 | II-1 | 78 |
| | AIN4=INT4 | II-1 | 79 |
| | BIN1=1-INT1 | II-1 | 80 |
| | BIN2=1-INT2 | II-1 | 81 |
| | BIN3=1-INT3 | II-1 | 82 |
| | BIN4=1-INT4 | II-1 | 83 |
| | U(I,J)=(AIN1*U1*DM1+AIN2*U2*DM2-AIN3*U3*DM3-AIN4*U4*DM4+UTD(I,J)* | II-1 | 84 |
| | 1(ROU(I,J)*VOL+BIN1*DM1+BIN2*DM2-BIN3*DM3-BIN4*DM4))/(VOL*ROUNP1) | II-1 | 85 |
| | V(I,J)=(AIN1*V1*DM1+AIN2*V2*DM2-AIN3*V3*DM3-AIN4*V4*DM4+VTD(I,J)* | II-1 | 86 |
| | 1(ROU(I,J)*VOL+BIN1*DM1+BIN2*DM2-BIN3*DM3-BIN4*DM4))/(VOL*ROUNP1) | II-1 | 87 |
| | E(I,J)=(AIN1*E1*DM1+AIN2*E2*DM2-AIN3*E3*DM3-AIN4*E4*DM4+ETD(I,J)* | II-1 | 88 |
| | 1(ROU(I,J)*VOL+BIN1*DM1+BIN2*DM2-BIN3*DM3-BIN4*DM4))/(VOL*ROUNP1) | II-1 | 89 |
| | EI(I,J)=E(I,J)-(U(I,J)**2+V(I,J)**2)/2. | II-1 | 90 |
| | ROU(I,J)=ROUNP1 | II-1 | 91 |
| | IF(EI(I,J).LT.0.) GO TO 440 | II-1 | 92 |
| | IF(I.GE.ISTP(J)) GO TO 470 | II-1 | 93M |
| | I=I+1 | II-1 | 94 |
| | GO TO 403 | II-1 | 95 |
| 416 | IF(J.EQ.JN) GO TO 500 | II-1 | 96 |
| | J=J+1 | II-1 | 97 |
| | GO TO 401 | II-1 | 98 |
| 440 | WRITE(6,450) I,J,ITIME,EI(I,J) | II-1 | 99 |
| 450 | FORMAT(1H0,38HINTERNAL ENERGY BECOMES NEGATIVE AT I= I4,3H J= I4, | II-1 | 100 |
| | 1 2OH AT TIME CYCLE NO.= I8, 9H EI(I,J)= E15.7) | II-1 | 101 |
| | GO TO 60 | II-1 | 102 |
| 470 | IF(ISTP(J).GE.IN) GO TO 472 | II-1 | 103M |
| | ISTP1=ISTP(J) | II-1 | 104M |
| | DO 471 I=ISTP1+1,IN | II-1 | 105M |
| | E(I,J)=EINF | II-1 | 106M |
| 471 | CONTINUE | II-1 | 107M |
| 472 | GO TO 416 | II-1 | 108M |
| C *** | *** | | |
| C *** | *** | | |
| C | II-2 THE TOTAL MASS AND ENERGY CALCULATION | II-2 | 1 |
| C *** | *** | | |
| C *** | *** | | |
| 500 | J=1 | II-2 | 2 |
| | SIGMM=0. | II-2 | 3 |
| | SIGME=0. | II-2 | 4 |
| | VOL=DR*DX | II-2 | 5 |
| 501 | IF(ITYPE.EQ.2) VOL=2. *PI*(FLOAT(J)-.5)*DX*DX**2 | II-2 | 6 |
| 502 | I=1 | II-2 | 7 |
| 503 | SIGMM=SIGMM+ROU(I,J)*VOL | II-1 | 8 |
| | SIGME=SIGME+ROU(I,J)*VOL*E(I,J) | II-1 | 9 |
| | IF(I.EQ.IN) GO TO 505 | II-1 | 10 |
| 504 | I=I+1 | II-1 | 11 |
| | GO TO 503 | II-1 | 12 |
| 505 | IF(J.EQ.JN) GO TO 600 | II-1 | 13 |
| | J=J+1 | II-1 | 14 |
| | GO TO 501 | II-1 | 15 |

| | | | |
|-------|--|--|---------|
| C *** | *** | | |
| C *** | *** | | |
| C *** | III | AUXILIARY CALCULATION AND DATA PLOT | III 1 |
| C *** | *** | | |
| C *** | *** | | |
| 600 | ETOT=SIGME | | III 2 |
| | DE=ETOT-ETH | | III 3 |
| | IF(ABS(DE/ETH).GT.EPSE) GO TO 603 | | III 4 |
| 601 | CMTOT=SIGMM | | III 5 |
| | DM=CMTOT-CMTH | | III 6 |
| | IF(ABS(DM/CMTH).GT.EPSM) GO TO 604 | | III 7 |
| 602 | ETH=ETOT | | III 8 |
| | CMTH=CMTOT | | III 9 |
| | T=FLOAT(ITIME-ITOFF)*DT | | III 10 |
| | IF(ITIME.GE.IDT) T=TOFF+T | | III 10A |
| | IF(MOD(ITIME,IPRINT).EQ.0) GO TO 700 | | III 11M |
| | GO TO 102 | | III 12 |
| 603 | WRITE(6,1111) | | III 13 |
| | WRITE(6,1000) | | III 14 |
| 1111 | FORMAT(1H0,15HENERGY CHECK |) | III 15 |
| 1000 | FORMAT(1H0,19X | ,5H ETH=E15.7,6H ETOT=E15.7,4H DE=E15.7) | III 16 |
| | GO TO 601 | | III 17 |
| 604 | WRITE(6,2222) | | III 18 |
| | WRITE(6,1001)CMTH,CMTOT,DM | | III 19 |
| 2222 | FORMAT(1H0,15HMASS CHECK |) | III 20 |
| 1001 | FORMAT(1H0,4HETH=E15.7,6H MTOT=E15.7,4H DM=E15.7) | | III 21 |
| | GO TO 602 | | III 22 |
| 605 | WRITE(6,15) T,ITIME,MEMR,ITYPE | | III 23 |
| | DO 606 J=1,JN | | III 25 |
| | WRITE(6,608) J | | III 26 |
| | WRITE(6,3333) | | III 24 |
| | ISTPPI=ISTPP(J) | | III 261 |
| | DO 607 I=1,ISTPPI | | III 27 |
| | ROU=ROU(I,J) | | III 28 |
| | EI=EI(I,J) | | III 29 |
| | ROU(I,J)=ROU(I,J)/ROINF | | III 30 |
| | EI(I,J)=EI(I,J)/EINF | | III 31 |
| | IF(MOD(I,2).EQ.0) GO TO 609 | | III 32 |
| | WRITE(6,1003)I, ROU(I,J),U(I,J),V(I,J),EI(I,J) | | III 33 |
| | GO TO 610 | | III 34 |
| 609 | WRITE(6,1004)I, ROU(I,J),U(I,J),V(I,J),EI(I,J) | | III 35 |
| 610 | ROU(I,J)=ROUM | | III 36 |
| | EI(I,J)=EIM | | III 37 |
| 607 | CONTINUE | | III 38 |
| 606 | CONTINUE | | III 39 |
| 15 | FORMAT(1H1,2HT=F12.6,16H TIME CYCLE NO.=I8,6H MEMR=I8,5H TYPEI8) | | III 40 |
| 3333 | FORMAT(1H0,2(60H | I ROU(I,J) U(I,J) V(I,J) | III 41 |
| | 1 EI(I,J))) | | III 42 |
| 608 | FORMAT(1H0,2HJ=I5) | | III 43 |
| 1003 | FORMAT(1H ,I8,4X,4F12.6) | | III 44 |
| 1004 | FORMAT(1H+,60X,I8,4X,4F12.6) | | III 45 |
| | IF(IPAR.NE.1) GO TO 102 | | III 45A |
| | WRITE(3) ITIME,IPRINT,CMTH,ETH,DT | | III 45B |
| | WRITE(3) ((ROU(I,J),U(I,J),V(I,J),EI(I,J),I=1,IN),J=1,JN) | | III 45C |
| | GO TO 102 | | III 46 |
| C *** | *** | | |
| C *** | *** | | |

```
C      III2 PRINT PAGE CONTROL ROUTINE
C *** ***
C *** ***
700 J=1
701 I=1
702 IF(ROU(I,J)-ROINF.LT.1.E-6) GO TO 703
      IF(I.GE.IN) GO TO 703
      I=I+1
      GO TO 702
703 ISTPP(J)=I
      IF(J.GE.JN) GO TO 605
      J=J+1
      GO TO 701
      END
```

| | |
|------|----|
| III2 | 1 |
| III2 | 2 |
| III2 | 3 |
| III2 | 4 |
| III2 | 5 |
| III2 | 6 |
| III2 | 7 |
| III2 | 8 |
| III2 | 9 |
| III2 | 10 |
| III2 | 11 |